15.3 LARGE EDDY SIMULATIONS ON THE EFFECTS OF SURFACE GEOMETRY OF BUILDING ARRAYS ON TURBULENT ORGANIZED STRUCTURES

Manabu Kanda *
Tokyo Institute of Technology, Tokyo, Japan

1. INTRODUCTION

Urban surface geometries are very complex. Thus, determining common features of turbulent flow structures above urban-like roughness is difficult. Actually, controversial observations related to the urban turbulent flow structures are found in the literature. Some papers noted that flow structures are similar to mixing layers or vegetation layers, which are dominated by sweep motions near the roughness (e.g., Raupach, 1981; Rotach, 1993). While another study determined a resemblance to flat-wall boundary layers, which are dominated by ejections and streaky patterns of longitudinal low speed regions (so called low speed streaks) exist (e.g., Osaka and Mochizuki, 1988; Antonia and Djendi, 1997; Kanda et al., 2004). Raupach et al. (1991) suggested that one possibility for these different flow structures over rough walls could be attributed to the different surface geometries such as D-type or K-type roughness, which is the concept proposed by Perry et al. (1969). However, the observed and simulated turbulent flow data above urban-like obstacles is limited. Thus, the major issues like what kinds of urban-like roughness can be classified into D-type or K-type and how they resemble to the mixing layers or flat-wall boundary layers still remain.

This study aims to investigate the effects of surface geometry of building arrays on the turbulent flow structures using Large Eddy Simulations. The temporal-mean wind profiles and the corresponding flow regimes in relation to surface geometries are well studied (Macdonald et al., 1998) and hence are not discussed here. The current focus is on turbulent structures such as drag coefficients, the relative contribution of sweep/ejections, and the visualized turbulent organized structures.

This study is directly motivated by Kanda et al. (2004) in which the numerical model used in the present (LES-CITY) was validated and the turbulent flow structures for square arrays of cubes were analyzed. In addition to the data of Kanda et al. (2004), a new series of simulation data including both square and staggered arrays with various area densities, mean building heights, and variable building heights are used. Thereby, allowing a general discussion.

* Corresponding author address: Manabu Kanda, Tokyo Institute of Technology, Dept. of International Development Engineering, Meguro-ku, O-okayama, 2-12-1 Tokyo, 152-8552 JAPAN; e-mail: kanda@ide.titech.ac.jp

2. NUMERICAL EXPERIMENTS

Kanda et al. (2004) described the LES model. Although the governing equations and the manner of turbulence closure are from Deardorff (1980), combining a masking method and a pressure solver with FFT is a very effective model for large eddy simulation of complicated airflow in cities. Simulations were performed for fully developed turbulent channel flows with building arrays on the bottom wall. The bottom surface geometry includes both square and staggered arrays with various area densities and building heights (**Table 1**).

Table 1 Computational conditions

RUN	λ_p	N_x	N_y	H_x	H_y	H_z	h	array	Grid Number
RUN P03	0.03	3	1	$18H$	$6H$	$6H$	H	square	182×62×62
RUN P11	0.11	6	2	$18H$	$6H$	$6H$	H	square	182×62×62
RUN P15	0.15	7	3	$18.2H$	$7.8H$	$6H$	H	square	184×80×62
RUN P20	0.20	8	3	$17.6H$	$6.6H$	$6H$	H	square	178×68×62
RUN P25	0.25	9	3	$18H$	$6H$	$6H$	H	square	182×62×62
RUN P30	0.30	10	4	$18H$	$7.2H$	$6H$	H	square	182×74×62
RUN P35	0.35	10	4	$17H$	$6.8H$	$6H$	H	square	172×70×62
RUN P44	0.44	12	4	$18H$	$6H$	$6H$	H	square	182×62×62
RUN S06	0.06	4	2	$18H$	$6H$	$6H$	H	staggered	162×82×62
RUN S11	0.11	6	2	$18H$	$6H$	$6H$	H	staggered	182×62×62
RUN S15	0.15	6	3	$15.6H$	$7.8H$	$6H$	H	staggered	158×80×62
RUN S20	0.20	8	3	$17.6H$	$6.6H$	$6H$	H	staggered	178×68×62
RUN S25	0.25	8	3	$18H$	$6H$	$6H$	H	staggered	162×62×62
RUN S35	0.35	10	4	$18H$	$7.2H$	$6H$	H	staggered	172×70×62
RUN S44	0.44	12	4	$18H$	$6H$	$6H$	H	staggered	182×62×62
RUN F11	0.11	6	2	$18H$	$6H$	$6H$	$1.4H$	square	182×62×62
RUN F25	0.25	9	3	$16H$	$6H$	$6H$	$1.4H$	square	182×62×62
RUN F44	0.44	12	4	$18H$	$6H$	$6H$	$1.4H$	square	182×62×62
RUN G11	0.11	8	3	$18H$	$6H$	$6H$	$0.6H$	square	182×68×62
RUN G25	0.25	8	3	$16H$	$6H$	$6H$	$0.6H$	square	162×62×62
RUN G44	0.44	12	4	$18H$	$6H$	$6H$	$0.6H$	square	182×62×62
RUN H11	0.11	10	4	$18H$	$6H$	$6H$	$H \pm 20\%$	square	182×62×62
RUN H25	0.25	8	3	$16H$	$6H$	$6H$	$H \pm 20\%$	square	162×62×62
RUN H44	0.44	12	4	$18H$	$6H$	$6H$	$H \pm 20\%$	square	182×62×62
RUN V11	0.11	10	4	$18H$	$6H$	$6H$	$H \pm 40\%$	square	182×62×62
RUN V25	0.25	8	3	$16H$	$6H$	$6H$	$H \pm 40\%$	square	162×62×62
RUN V44	0.44	12	4	$18H$	$6H$	$6H$	$H \pm 40\%$	square	182×62×62

To see the effects of non-uniform building heights, equal increment and decrement of ± 20 % and ± 40 % about the mean height (H= 50m) are assigned to alternate obstacles. The horizontal cross-section of each building is a 50 m x 50 m square, the grid spacing is 5 m, and the time step is 0.1 s. Adjusting the height-independent longitudinal pressure gradient at each time step maintained the average longitudinal velocity across the y-z cross-section at 1.0 m s-1. Periodic boundary conditions apply in the stream-wise (x) and span-wise (y) directions. For all solid surfaces, the local profile of the tangential velocity component is considered logarithmic and the normal velocity component is zero. The local roughness scale is assumed constant at 0.01 m. Each simulation lasted for 360,000 time steps, which ensures that the flow is quasi-steady with fully-developed turbulence. The

results from the last 7,2000 time steps are used for all investigations. Table I summarizes the experimental conditions.

3. RESULTS AND DISCUSSION

3.1 DRAG COEFFICIENT

Drag coefficients C_d are used to measure the aerodynamic surface properties of building arrays instead of roughness parameters such as roughness length and displacement height since recent studies noted the uncertainty in the regression of these conventional parameters (Iyengar and Farell, 2001; Cheng and Castro, 2002; Kanda et al., 2004).

The drag coefficients used in the analysis below are calculated at the height where Reynolds stress shows a peak value, which coincides with the building tops in most cases, except for the square arrays with alternating building heights. Interestingly, Reynolds stress for non-uniform building heights have the peak values at the top of the higher buildings not at the mean height shown in **Figure 1**.

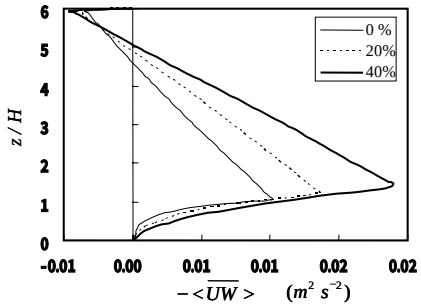

Fig.1 Effect of non-uniform building height on the vertical profile of temporally and horizontally averaged Reynolds stress. The solid, dotted, and bold lines represent uniform cubes (RUN P44), buildings with 20 % height variations (RUN H44), and buildings with 40 % height variations (RUN V44), respectively. All results are for square arrays of buildings with area density = 0.44.

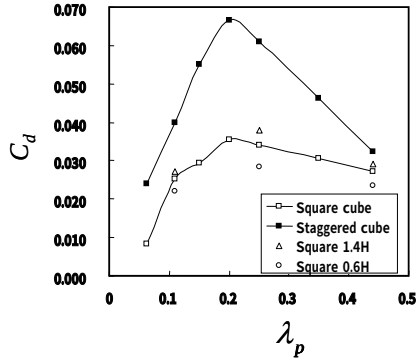

Fig.2 temporally and horizontally averaged drag coefficients for uniform-building arrays in relation to the building area density. The white and black squares represent the square and staggered cube arrays, respectively. The triangles and circles are the square arrays of the taller and shorter buildings, respectively.

Comparing the results of the square and staggered 'cube' arrays, demonstrates that the values of C_d for the staggered arrays tend to be higher and more sensitive to cube area density, while those for square arrays are insensitive to area density (**Figure 2**). In contrast to the familiar manner of sensitive C_d to area density as shown in the results of staggered arrays, the broad peak of C_d to area density for square arrays are not concise. However, the laboratory data of Macdonald et al. (1998) observed the same tendency. Perry et al. (1969) proposed two types of surface roughness. One is D-type roughness where C_d depends on an outer scale such as the boundary layer height and is independent of the roughness scale. The other is K-type roughness where depends on the roughness scale. Although the two types of roughness are extreme concepts and intermediate forms can exist, according to Perry's classification, the square and staggered building arrays can be successfully classified into D-type and K-type roughness, respectively.

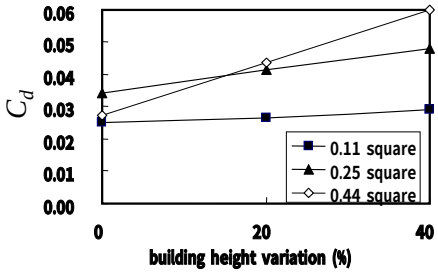

Fig.3 The effect of building height variations (0 %, 20 % and 40 %) on the drag coefficients for area density = 0.11 (black square), 0.25 (black triangle) and 0.44 (white diamond) . All results are for square arrays of buildings.

This simple classification appears not to apply to dense square arrays with a variety of building heights. The drag coefficient for area density = 0.44 becomes proportionally larger with the variations in building height, but area density = 0.11 is insensitive to height variations (**Figure 3**). These results are consistent with the laboratory experiment of Macdonald et al. (1998). For area density = 0.44, the array with 40 % variation in building height gives a much larger C_d than the arrays with uniform building height of h=1.4H (**Figure 2** and **Figure 3**). Thus, the enhancement cannot be explained by only ignoring the existence of lower buildings, which implies that the height variability in dense arrays directly modifies the turbulent flow structure near the top of taller buildings where strong wind shear layers and the resulting peak of Reynolds stress are produced. Louka et al's field experiments (1998) demonstrated that the geometries of shallow pitched roofs influence the eddy structure near the roof level.

3.2. RELATIVE CONTIBUTION OF EJECTION AND SWEEP

Momentum fluxes can be divided into four components based on the signs of the streamwise and vertical velocity fluctuations from the temporal-means (u' and v'). Ejections (quadrant 2) and sweeps (quadrant 4) play a significant role in turbulent boundary layer dynamics. The stress fraction S_i for quadrant 'i' is defined as the flux contribution to Reynolds stress from that quadrant, and the time fraction T_i is the duration of that event relative to the total integration time. The absolute values of S_i and T_i are inadequate for flow classification since T_i is not very sensitive to the surface nature (Katul et al., 1997), and S_i depends on the roughness type (Krogstad et al., 1992). The relative contribution of stress (S_2/S_4) and time (T_2/T_4) of ejections to sweeps (Lu and Willmarth, 1973), which are indices for qualifying turbulent structures, are a better alternative for classifying flow. Ejections are more intense in flat-wall boundary layers or D-type roughness ($S_2/S_4 > 1$ and $T_2/T_4 < 1$; Krogstad et al., 1992; Osaka and Mochizuki, 1988; Kanda et al, 2004) while sweeps are dominant in vegetation layers or K-type roughness ($S_2/S_4 < 1$ and $T_2/T_4 > 1$; Gao et al. 1989; Nakagawa and Nezu, 1977; Raupach, 1981). The relative contribution of sweeps and ejections at the cube height differ for square and staggered cube arrays (**Figure 4**).

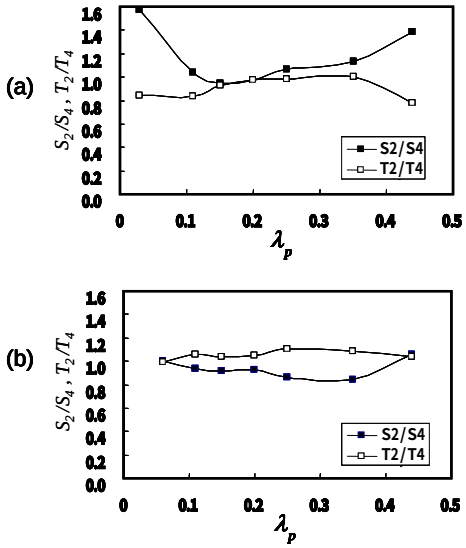

Fig.4 The relative contributions of ejections to sweeps for stress S_2/S_4 (black) and their time fraction T_2/T_4 (white) in relation to the building area density. (a) square cube arrays and (b) staggered cube arrays

S_2/S_4 for square arrays are sensitive to building area density and are almost equal to or larger than 1.0 (ejection dominant), while those for staggered arrays are insensitive to building area density and are less than 1.0 (sweep dominant). The sensitivity of S_2/S_4 to area density in square cube arrays is attributed to the mixed properties of the two different turbulent flows since the flow along the street line behaves like a flat-wall boundary layer, while that along the roofline acts like a mixing layer. In contrast, the turbulent flow in staggered arrays behaves like a mixing layer throughout the domain.

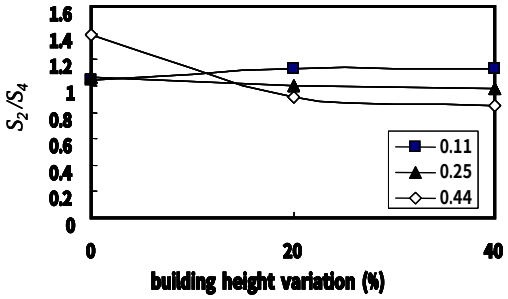

Fig.5 The effect of building height variations (0 %, 20 % and 40 %) on S_2/S_4 for area density = 0.11 (black square), 0.25 (black triangle) and 0.44 (white diamond). All results are for square arrays of buildings.

The effect of height variations on the quadrant statistics is more significant for denser square arrays (**Figure 5**), which qualitatively corresponds to the drag coefficients (**Figure 3**). Note that the quadrant statistics are calculated at the height of the taller buildings where Reynolds stress is maximized. In dense square arrays of area density = 0.44, the relative contribution of ejections to sweeps becomes smaller as the variations in building height increase and the value of S_2/S_4 with 40 % building height variation is the smallest compared to those for any square and staggered cube arrays with uniform building heights. This suggests that the height variability in dense arrays effectively intensifies the shear layer along the rooflines. In contrast, the value of S_2/S_4 for sparse square arrays of area density = 0.11 is insensitive to height variations.

3.3. TURBULENT ORGANIZED STRUCTURES

Visualization of turbulent organized structures (TOS) is a direct measurement for identifying the flow. 'Low speed streaks' and 'rollers' are distinctive TOS observed in flat-wall boundary layers and in mixing layers, respectively. The low speed streaks are defined as regions where the streamwise velocity fluctuations from the horizontal mean are negative and are usually longitudinally-elongated. The rollers are defined as two-dimensional large clumps of spanwise vorticity extending in the spanwise direction. TOS of square cube arrays and staggered cube arrays are visualized in **Figures 6** and **7**. Note that all of these figures are representatively depicted for area density = 0.25, but the following discussions are true for other area densities as well. Surprisingly, low speed streaks are observed, but rollers are not in all of the present simulations. The common features of simulated TOS are summarized as follows. (1) Low speed streaks are longitudinally extended to the scale

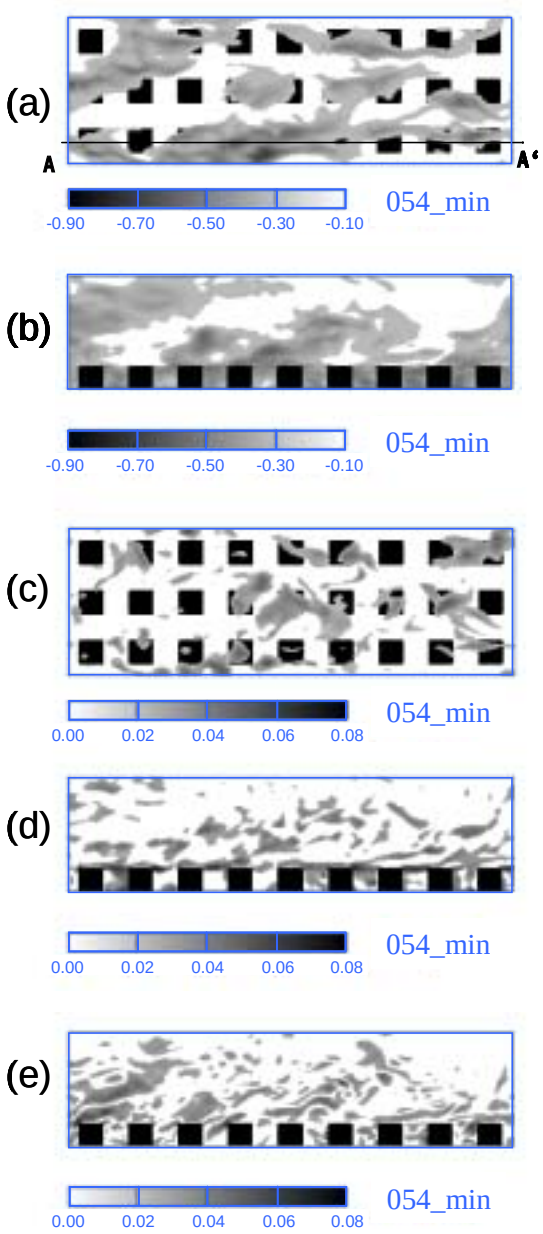

Fig.6 Instantaneous images of turbulent organized structures for the square cube array with area density = 0.25 (RUN P25). The flow is left to right. (a) horizontal cross-section of low speed streaks, which is defined as the region where the streamwise velocity fluctuation is negative, (b) vertical cross-section of low speed streaks, (c) horizontal cross-section of spanwise vorticity component, (d) vertical cross section of spanwise vorticity component, and (e) vertical cross-section of streamwise vorticity component. The position of y for the cross-section in (b), (d) and (e) is indicated by A-A' in (a).

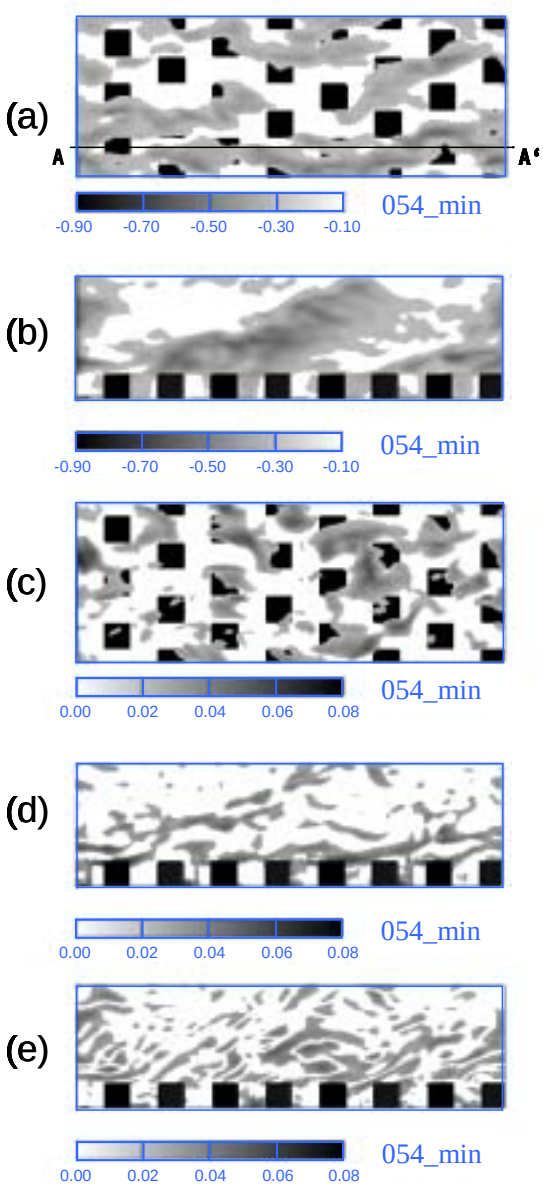

Fig.7 Same as Figure6, but is for the staggered cube arrays with are density = 0.25 (RUN S25).

of 10-20H (**Figures 6a** and **7a**) and are lifted downstream up to 4-5H elevation (**Figures 6b** and **7b**). (2) Rollers are not found and the coherence of spanwise vorticity in the spanwise direction is poor (**Figures 6c** and **7c**). (3) Clusters of shorter vortices correspond to the larger low speed streaks. The spanwise vortices are lifted downstream along the upper edge of the low speed streaks (**Figures 6d** and **7d**) and the streamwise vortices are more steeply lifted downstream (**Figures 6e** and **7e**). These

characteristics of TOS are consistent with the 'hairpin vortex packet model' as proposed in Adrian et al. (2000), although the packet structures have been discussed only for flat-wall boundary layers and not for rough-wall boundary layers.

Low speed streaks have been observed over D-type roughness flows (Osaka and Mochizuki, 1988; Antonia and Djendi, 1997), in atmospheric surface layers (Hommema and Adrian, 2003) and over smooth walls (e.g., Kline et al., 1967; Robinson, 1991). Therefore, the existence of low speed streaks in square cube arrays is expected as part of the D-type roughness classification. In contrast to the sweep dominated statistics, which imply that low speed streaks are unlikely to be found over K-type roughness (Raupach et al., 1991; Antonia and Djendi, 1997), low speed streaks are commonly present in K-type like roughness such as staggered cube arrays. This new finding supports the previous LES results of Kanda et al. (2004) that TOS of urban-like flows more closely resembles those of wall turbulent layers and differs from those of vegetation-like flows, which are represented by rollers (Gao et al., 1989; Kanda and Hino, 1994).

Although the nested packet structures of shorter vortices that generate large low speed streaks are common, differences in TOS between D-type (square cube arrays) and K-type (staggered cube arrays and square building arrays with height variation) are found. The low speed streaks and the corresponding shorter vortices for the K-type roughness are more extended and more steeply inclined downstream than D-type roughness counterparts (**Figures 6** and **7**). A possible reason for this is that the damping of vertical motion along the strong shear layers at the rooflines is not as severe for K-type roughness due to the open nature of the roofline geometry. The larger vertical motions will intensify the lift of strong shear layers, which produce the steeper ejections above and the stronger sweeps near the canopy top.

Table 2 summarizes the contrastive turbulent structures of the square and staggered cube arrays for the D- and K-type roughness, respectively. The square building arrays with height variations are not included in the table, however, they belong to the K-type roughness. Note that the Perry's classification (D- and K-type roughness) has been used only with respect to the sensitivity of the drag coefficient to the surface geometry.

3.4 DIFFERENCE FROM VEGETATION FLOWS

Another question is what causes the differences in TOS of urban-like flows and vegetation-like flows. Both flows have an inflection point in the mean wind velocity profile due to the drag of the roughness elements. Thus, these canopy flows can inherently produce the shear instability (Ho and Huerre, 1984), unlike flat-wall boundary layers, which require an auto-generation mechanism to create shear instability (Schoppa and Hussain, 2002). Nevertheless, the disturbance produced by the shear instability can reach the self-similar form such as the large roller structures in vegetation flows, but not urban-like flows. The scale of each roughness element relative to the roughness layer height could be responsible for this essential difference. Many of the finer roughness elements such as leaves in vegetation layers can supply spatially, quasi-continuous vortex layers, while the vortex sheets produced by the buildings are more or less discontinuous, which greatly restricts spatial growth disturbances. Kanda et al. (2004) suggested that the various normalized turbulent statistics over urban-like obstacles differ from those over vegetation-like obstacles. **Table 3** lists the quadrant statistics (S_2/S_4) observed in real urban boundary layers. The values of S_2/S_4 at the height where the Reynolds stress marks the peak value are plotted using the manner of the present simulation results when building height varied. For some sites sweeps are dominant (Oikawa and Meng, 1994; Feigenwinter et al., 1999), but in others, ejections are dominant (Rotach, 1993; Moriwaki and Kanda, 2004). Although it is difficult to relate these values to the urban geometries from the limited data, it is noteworthy that the observed values range around 1.0 between 0.8-1.2, but those observed over vegetation canopies can take much smaller values around 0.5 (Show et al., 1983). The urban values near 1.0 even in the sweeps dominant range seem to reflect the absence of large rollers, which are predicted in the present LES.

REFERENCES

Adrian, R.J., Meinhart, C.D. and Tomkins, C.D. : 2000, 'Vortex Organization in the Outer Region of the Turbulent Boundary Layer', J.Fluid Mech., 422, 1-54.

Antonia, R. A. and Djendi, L.: 1997, 'Reynolds Stress Producing Motions in Smooth and Rough Wall Boundary Layers', in R. L. Panton (ed.), Self-Sustaining Mechanisms of Wall Turbulence, Advances in Fluid Mechanics 15, Computational Mechanics Publications, Southampton, 181–199.

Deardorff, J.W. : 1980, 'Stratocumulus-topped Mixed Layers Derived from a Three-dimensional Model', Boundary-Layer Meteorol. 18, 495–527.

Cheng, H. and Castro, I.P. : 2002, 'Near Wall Flow over Urban-like Roughness', Boundary-Layer Meteorol. 104, 229-259.

Feigenwinter, C., Vogt, R. and Parlow, E.: 1999,'Analysis of Organized Structure in Urban Turbulence', Biometeorology and Urban Climatology at the turn of the Millennium, 565-568.

Gao, W., Shaw, R.H., and Paw U, K.T. : 1989, 'Observation of Organized Structure in Turbulent Flow within and above a Forest Canopy', Boundary-Layer Meteorol. 47, 349-377.

Ho, C-M. and Huerre, P. : 1982, 'Perturbed Free Shear Layers', Ann.Rev.Fluid Mech., 16, 365-424.

Hommema, S.E. and Adrian, R.J.: 2003, 'Packet Structure of Surface Eddies in the Atmospheric Boundary Layer', Boundary-Layer Meteorol. 106,

147-170.
Iyengar, A.K.S. and Farell, C. : 2001, ‘Experimental Issues in Atmospheric Boundary Layer Simulations : Roughness Length and Integral Length Scale Determination’, J. Wind Eng. Ind. Aerodyn. 89, 1059-1080.
Kanda, M. and Hino, M. : 1994, ‘Organized Structures in Developing Turbulent Flow within and above a Plant Canopy, using a Large Eddy Simulation’, Boundary-Layer Meteorol. 68, 237-257.
Kanda, M., Moriwaki, R. and Kasamatsu, F.: 2004, ‘Large Eddy Simulation of Turbulent Organized Structure within and above Explicitly Resolved Cube Arrays’, Boundary-Layer Meteorol. (in press)
Katul, G., Hsieh, C-I., Kuhn, G. and Ellsworth, D. : 1997, ‘Turbulent Eddy Motion at the Forest-atmosphere Interface’, J.Geophys.Res, 102, 13,409-13,421.
Kline, S. J., Reynolds,W. C., Schraub, F. A., and Runstadler, P.W.: 1967, ‘The Structure of Turbulent Boundary Layers’, J. Fluid Mech. 30, 741–773.
Krogstad, P., Antonia, R.A. and Browne, L.W.B. : 1992, ‘Comparison between Rough- and Smooth-wall Turbulent Boundary Layers’, J. Fluid Mech. 245, 599-617.
Louka P., Belcher, S.E. and Harrison, R.G. : 1998, ‘Modified Street Canyon Flow’, J. Wind Eng. Ind. Aerodyn. 74-76, 485-493.
Lu, S.S. and Willmarthe, W.W. : 1973, ‘Measurements of the Structure of the Reynolds Stress in a Turbulent Boundary Layer’, J. Fluid Mech., 60, 481-571.
Nakagawa, H. and Nezu, I.: 1977, ‘Prediction of the Contributions to the Reynolds Stress from Bursting Events in Open-channel Flow’, J. Fluid Mech., 80, 99-128.
Macdonald, R.W., Hall, D.J., Walker, S. and Spanton, A.M. : 1998, ‘Wind Tunnel Measurements of Windspeed Within Simulated Urban Arrays’, BRE Client Report CR 243/98, 62pp.
McNaughton, K.G. and Brunet, Y. : 2002, ‘Townsend’s Hypothesis, Coherent Structures and Monin-Obukhov Similarity’, Boundary-Layer Meteorol. 102, 161-175.
Oikawa, S. and Meng, Y. : 1995, ‘Turbulence Characteristics and Organized Motion in a Suburban Roughness Sublayer’, Boundary-Layer Meteorol., 74, pp.289-312.
Osaka, H. and Mochizuki, S. : 1988, ‘Coherent Structure of a D-type Rough Wall Boundary Layer’, In Transport Phenomena in Turbulent Flows: Theory, Experiment and Numerical simulation (ed. M.Hirata and N.Kasagi), 199-211, Hemisphere.
Perry, A.E., Schofield, W.H. and Joubert, P.N. : 1969, ‘Rough Wall Turbulent Boundary Layers’, J. Fluid Mech., 37, 383-413.
Raupach, M.R. : 1981, ‘Conditional Statistics of Reynolds Stress in Rough-wall and Smooth-wall Turbulent Boundary Layers’, J. Fluid Mech., 108, 363-382.
Raupach, M.R., Antonia R.A. and Rajagopalan, S.: 1991, ‘Rough-wall Turbulent Boundary Layers’, Appl. Mech. Rev. 44, 1-25.
Robinson, S. K.: 1991, ‘Coherent Motions in the Turbulent Boundary Layer’, Annu. Rev. Fluid Mech. 23, 601-639.
Rotach, M.W.: 1993, ‘ Turbulence Close to a Rough Urban Surface Part Ⅰ Reynolds Stress, Boundary-Layer Meteorol. 65, 1-28.
Schoppa, W. and Hussain, F. : 2002, ’Coherent Strucure Generation in Near-wall Turbulencce’, J. Fluid Mech., 453, 57-108.
Shaw, R.H., Tavangar, J. and Ward, D.P. : 1983, ‘Structure of the Reynolds Stress in a Canopy Layer’, J.Clim.Appl.Meteoro. 22, 1922-1931.
Townsend, A.A : 1976, The Structure of Turbulent Shear Flow. Cambridge University Press. 429 pp.